MEDICINE UPDATES JOURNAL
Faculty of Medicine Port Said University
Volum: 19 No:3 PP:36 - 54

# "Correlation of Ultrasound Features in the TIRADS Scoring System with Cytological Findings in the FNAC of Thyroid Nodules "

**Authors**

Carmen Ali Zarad [1], Mohamed Elrakhawy [2], Waleed Said Abo Shanab [1], Amr Abo elfarh [3], Khaled Abd El-Baky Ahmed [1]

[1] Diagnostic Radiology, Faculty of Medicine- Port Said University
[2] Diagnostic Radiology, Faculty of Medicine - Mansoura University
[3] Radiology Department, Suez Canal Authority, Port Said

**Submitted: 08/07/2024**
**Accepted:09/08/2024**

**DOI: 10.21608/muj.2024.302695.1175**

**ISSN : 2682-2741**



**https://muj.journals.ekb.egdean@med.psu.edu.eg**
**vice_dean_postgraduate@med.psu.edu.eg**

## ABSTRACT:

***Background:*** According to American College of Radiology—Thyroid Association guidelines, ultrasound is the imaging modality of choice for examination.

Ultrasonographic examination detects the thyroid nodules, determines their size, number, and character, and assists in cytological assessment by guiding fine needle aspiration cytology of worrisome nodules.

Thyroid Imaging Reporting and Data System is a scale for risk stratification based on well-defined ultrasonography characteristics.

**Aim of the study:**

We aimed to distinguish between benign and malignant thyroid nodules using an ultrasound-based stratification approach.

**Materials and methods:**

The study was conducted between January 2022 and March 2024. It included 70 patients (43 female and 27 male) with thyroid nodules. Each patient's thyroid gland nodules were examined via an ultrasound-based scoring system with fine needle aspiration cytology from the most significant nodule.

**Results:**

This prospective study included 70 patients with thyroid nodules. Of this population, 41 patients (58.6%) had benign thyroid nodules, and 29 patients (41.4 %) had malignant thyroid nodules.

The Thyroid Imaging Reporting and Data System showed 80.80% sensitivity, 77% specificity, 72.5% positive predictive value, and 74.3% negative predictive value in the evaluation of thyroid nodules with increased malignancy risk as the final TIRADS category increased from 1 to 5 (P value < 0.001).

**Conclusions:**

The Thyroid Imaging Reporting and Data System is an ultrasound-based method with high diagnostic accuracy for discriminating between benign and malignant thyroid nodules.

**Keywords:**

Fine needle aspiration cytology, Thyroid nodules, Thyroid Imaging Reporting and Data System, Ultrasound.

# Background

Ultrasonographic examination detects thyroid nodules and determines their size, number, and character. It also assists cytological assessment by guiding fine needle aspiration cytology (FNAC) of worrisome nodules. **(1)**

The evaluation of ultrasound (US) features in five categories, composition, echogenicity, shape, margin, and echogenic foci, is the basis of the American College of Radiology (ACR) Thyroid Imaging Reporting and Data System (TI-RADS). Each feature is assigned a score between 0 and 3 (Fig 44). **(2)**

**I. Composition:**

Nodules classified as spongiform are considered benign, and no follow-up is required. Most scholars agree that the term "spongiform" describes the presence of minute cysts. **(2)**

The solid classification should be applied to nodules with cystic components comprising less than 5% of the total volume. **(3)**

**II. Echogenicity:**

The majority of the nodule's echogenicity determines its overall echogenicity. Nodule echogenicity can be classified as markedly hypoechoic (about the nearby strap muscle), hypoechoic, isoechoic, and hyperechoic (about the thyroid parenchyma). **(4)**

If a nodule's echogenicity cannot be determined due to dense calcification, it receives 1 point in this category and should be considered at least isoechoic or hyperechoic. **(4)**

**III. Shape:**

The shape is either taller than wide or wider than tall. On an axial scan, a nodule's width describes the transverse dimension, while its tallness is for its anteroposterior dimension. **(5)**

Malignant nodules grow in a centrifugal pattern across the normal tissue plane, whereas benign nodules grow in a parallel pattern along the tissue plane**.** A taller-than-wide form is highly suggestive of malignancy. **(6)**

### IV. Margin:

The nodule's margin is defined by its contact with surrounding intra- or extra-thyroidal tissue. There are several types of nodule margins: smooth, speculated/ irregular, lobulated, or poorly defined. **(7)**

A gradually curved interface characterizes a smooth edge. Both lobulated and irregular margins (invasion into the surrounding thyroid tissue) earn 2 points, so the distinction isn't critical. **(8)**

Three points are assigned for the extrathyroidal extension and invasion of adjacent structures. If the boundary is not depicted clearly, the nodule is labeled as ill-defined and receives zero points. **(8)**

### V. Echogenic foci:

Microcalcifications are punctate echogenic foci that are 1 mm or smaller and are assigned 3 points on the scale. Macrocalcifications, which are bigger than 1 mm, and rim calcifications, which are assigned 2 points**,** are assigned one point. **(9)**

Microcalcifications in the US are strongly suggestive of malignancy. Both benign and malignant nodules can have large, irregularly shaped dystrophic calcifications that can form due to tissue necrosis. **(10)**

Some punctate echogenic foci (PEF) within nodules do not actually represent microcalcifications, just as the echogenic material with reverberation artifacts associated with colloid, the posterior enhancement of tiny cysts, and the speckle pattern of normal or non-malignant thyroid tissue**. (11)**

The scoring of multiple types of echogenic foci is obtained by summating the points for each type. This contrasts with the other categories, where the highest-scoring finding is utilized to decide the point assignment for that characteristic. **(11)**

**<u>Calculation of total points for each thyroid nodule with recommendations for each thyroid nodule (Fig. 1):</u>**

Each feature is given a score between 0 and 3 for each category. The nodule's risk of malignancy is determined by its final TIRADS level, which ranges from benign (TIRAD I—0 points) to not suspicious (TIRAD II—2 points), mildly suspicious (TIRAD III—3 points), moderately suspicious (TIRAD IV—4 to 6 points), and highly suspicious (TIRAD V—7 points or more). **(12)**

Every report is required to give management suggestions on whether follow-up US is required or not, or whether it goes further to FNAC**:** TIRAD I & II: No FNA is required. TIRAD III: either ≥ 15 mm follow-up or ≥ 25 mm FNAC. TIRAD IV: either ≥ 10 mm follow-up or ≥ 15 mm FNAC. TIRAD V: either ≥ 5 mm follow-up or ≥ 10 mm FNAC. **(12)**

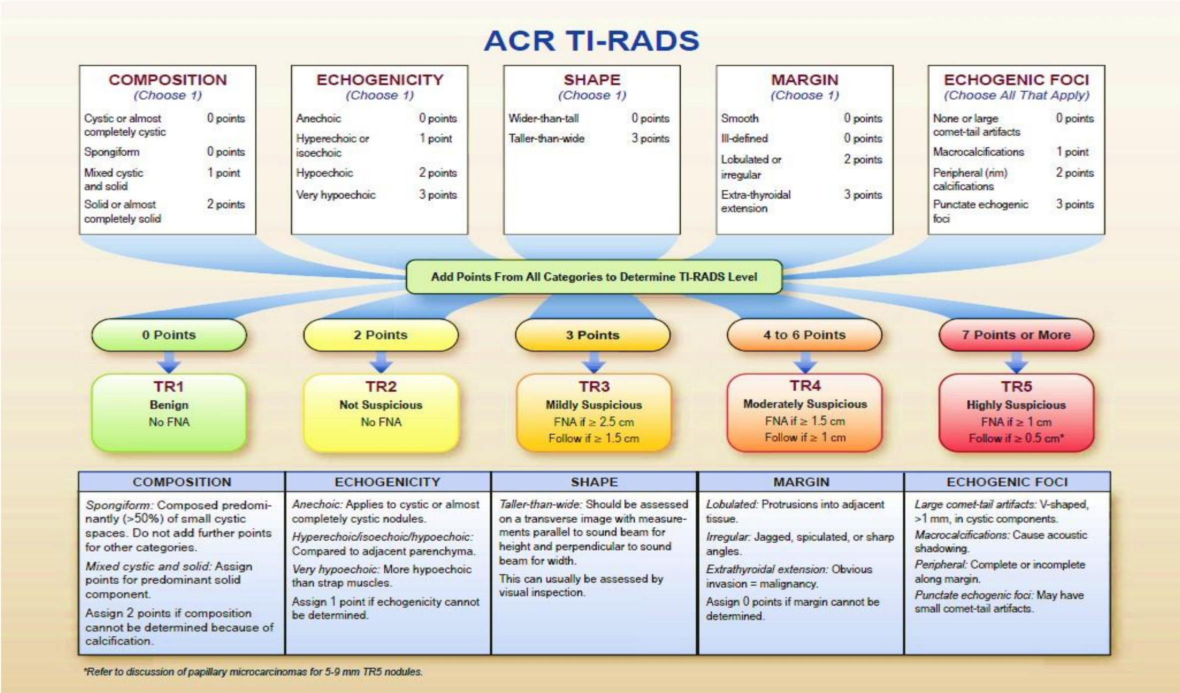


Fig. (1) shows the calculation of the total score and recommendation (quoted from ACR TI-RADS ATLAS TIRADS Classification (2020).**(11)**

## Aim of work:

Our objective was to distinguish between benign and malignant thyroid nodules using an ultrasound-based stratification approach (ACR TI-RADS) with correlation to FNAC.

# Materials and Methods

## Patients:

This prospective study was conducted between January 2022 and March 2024. It included 70 patients (43 female and 27 male) with thyroid nodules. Their mean age was 46.90±11.43 years, with a range of 20 to 70 years. Each patient's thyroid gland nodules were examined via ultrasonography. Every patient was intended to have FNAC.

The study had approved by our local committee of research and ethics and before participation, each subject signed an informed consent form.

## Inclusion criteria:

- Patients with thyroid nodules (the presence of solitary or multiple nodules, either solid or complex nodules.
- Post-operative thyroidectomy with local recurrent masses.

## Exclusion criteria:

- Pure thyroid cystic lesions.
- Diffuse thyroid diseases.
- Thyroid abscess.
- Patients who are ineligible for FNAC (e.g., Bleeding disorders).

## Ultrasound examination:

- For this investigation, a GE Logiq P7 ultrasound machine with a 9:12 MHz bandwidth linear transducer (L6-12-RS) was used in every case.
- The patients were lying down. To get the neck to hyperextend, a pillow was positioned behind the shoulders.
- All three planes of the thyroid gland were scanned using a linear transducer (longitudinal, transverse, and multiple obliques).
- A Doppler examination was conducted to evaluate the vascularity of the gland.
- We checked for nodules in each lobe and isthmus.
- TIRADs were assigned to each thyroid nodule after they were precisely measured and evaluated for echogenicity, composition, margin, shape, and echogenic foci.

**Ultrasound-guided FNAC**

- Bleeding profile tests which required an acceptable INR of up to 1.4 and a platelet count greater than 50,000/mL.
- US guidance with high-frequency probes, supine patient, and hyperextended head. The patient should be instructed not to swallow or speak when the needle is below the skin surface.
- Local anesthetics are rarely utilized because injections cause pain similar to that from biopsies. Additionally, anesthesia can change the smear's quality and reduce target site visibility in the US.
- An antiseptic is applied to the probe's surface.
- The needle's path to the intended nodule is identified.
- Using 25-27 gauge needle and syringe 5–10 mL.

- On the US screen, the needle's motion is detected and introduced to the target nodule either from the side of the probe, where it appears as an echogenic line, or in the middle of the probe, where it appears as an echogenic dot.
- After taking a sample from the most suspicious area and from the cyst's solid component, the sample was spread out on a glass slide, smeared, and sent for cytology.
- To stop bleeding, the puncture site is squeezed for 10 to 15 minutes with a sterile bandage.

**Statistical analysis and package:**

- After revision, coding, tabulation, and introduction to a PC, the gathered data was processed through the Statistical Package for Social Science (SPSS version 22).
- Quantitative variables are expressed as mean and SD or median and interquartile range (IQR) depending on the data distribution. Frequencies and percent's are used to express qualitative characteristics.
- Using the Student t-test and Mann-Whitney test, two study groups were compared on a continuous variable. The association between the categorical variables will be investigated using the chi square test. P-values less than 0.05 were regarded as statistically significant.
- Sensitivity, specificity, predictive value, and accuracy of the TIRADS level compared to the result of Ultrasound-guided FNAC of the thyroid nodules will be calculated.

# Results

Seventy patients with 70 thyroid nodules were enrolled in this prospective study and underwent US examination with TIRADS scoring and pathological examination by FNAC under ultrasound guidance.

Among our studied population, 42.9% were solid, 31.4% were mixed cystic/solid, and the remaining 25.7% were spongiform. Echogenicity was hyper or isoechoic in 41.4%, anechoic and hypoechoic in 21.4% for each, and very hypoechoic in 15.7%. The shape was wider than tall in 71.4% and taller than wide in 28.6%. The margin was smooth/ill-defined in 37.1%, lobulated/irregular in 32.9%, and extra-thyroid extension was detected in 30%. Macro calcification was detected in 18.6%, peripheral calcification in 5.7%, and punctate calcification in 7.1%. The total points given to the nodules ranged from zero to 14 points (Table 1).

In the malignant group compared to the benign group, our study revealed a statistically significant increase in the presence of solid composition, very hypoechoic echogenicity, taller than wide shape, lobulated or irregular margins, extra thyroidal extension, and micro calcifications.

Table (1): Ultra-sonographic findings of participating subjects (no. 70).

| Characteristics | No. | % |
|---|---|---|
| Composition | | |
| Spongiform | 18 | 25.7% |
| Mixed cystic/solid | 22 | 31.4% |
| Solid | 30 | 42.9% |
| Echogenicity | | |
| Anechoic | 15 | 21.4% |
| Hyper or isoechoic | 29 | 41.4% |
| Hypoechoic | 15 | 21.4% |
| Very hypoechoic | 11 | 15.7% |
| Shape | | |
| Wider than tall | 50 | 71.4% |
| Taller than wide | 20 | 28.6% |
| Margin | | |
| Smooth/ill-defined | 26 | 37.1% |
| Lobulated/irregular | 23 | 32.9% |
| Extra-thyroid extension | 21 | 30% |
| Echogenic foci | | |
| None | 48 | 68.6% |
| Macro calcification | 13 | 18.6% |
| Peripheral calcification | 4 | 5.7% |
| Punctate calcification | 5 | 7.1% |

Forty-one patients (58.6%) in our study group had benign thyroid nodules, which included eight patients (11.4%) with lymphocytic thyroiditis (Fig.2), 12 patients (17.1%) with colloid nodules (Fig.3), and 21 patients (30%) with follicular adenomas (Fig.4). In contrast, 29 patients (41.4%) had malignant thyroid nodules, which included two patients (2.9%) with B-cell lymphoma (Fig. 5), two patients (2.9%) with medullary carcinoma, seven patients (10%) with follicular carcinoma (Fig. 6), four patients (5.7%) with papillary carcinoma on top of follicular adenoma, and 14 patients (20%) with papillary carcinoma (Table 2).

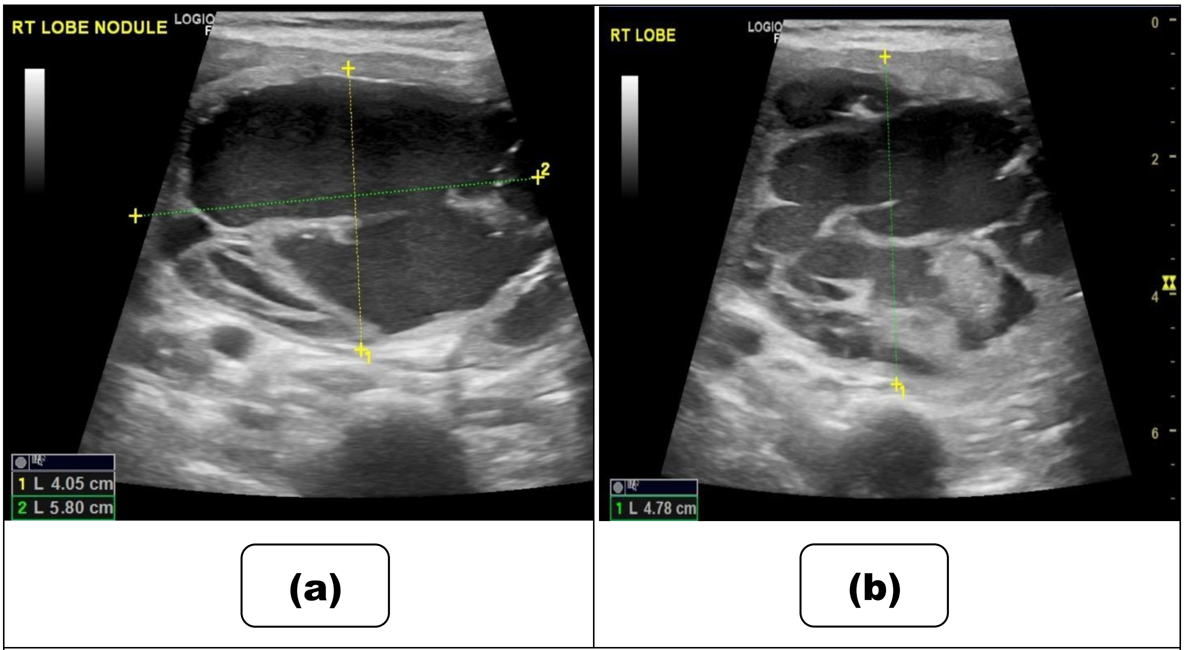


**Fig. (2):** Ultrasound images of lymphocytic thyroiditis (a, b).

- Asymmetrically enlarged both thyroid lobes with multiple nodules, the most significant nodule was seen at right lobe measuring about 40 x 58 mm (AP x T).
- TIRAD classification:

| Category | Comment | Score |
|---|---|---|
| Composition | Cystic | 0 |
| Echogenicity | Anechoic | 0 |
| Shape | Wider-than-tall | 0 |
| Margin | Smooth | 0 |
| Calcification | No | 0 |
| **Total** | | zero |

- Total score: zero …… TIRADS…I.

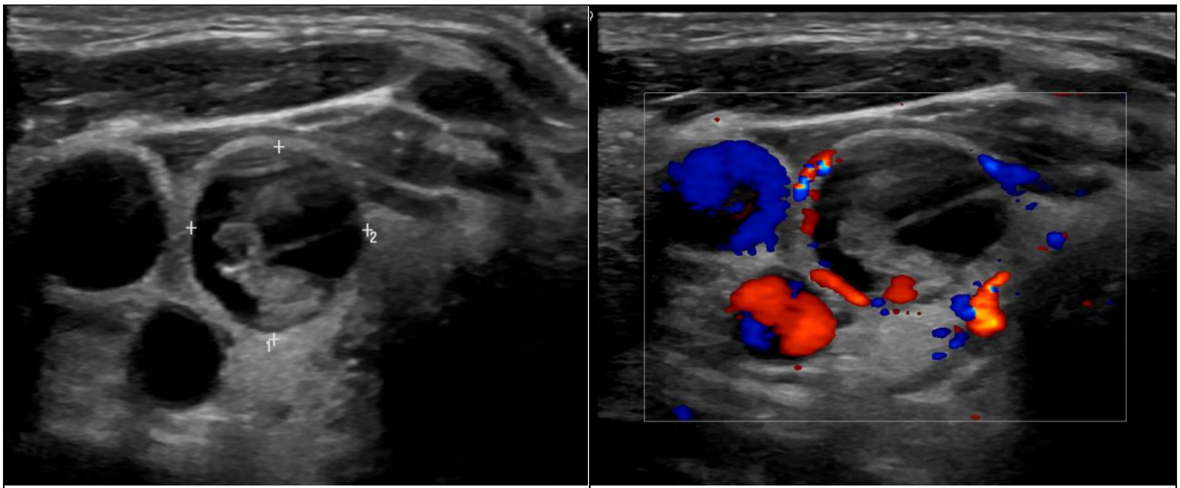

(a) (b)

**Fig. (3):** Ultrasound images of colloid cyst (a, b).

- Enlarged right thyroid lobe with nodule measuring about 11x12 mm (AP x T).
- TIRAD classification:

| **Category** | **Comment** | **Score** |
|---|---|---|
| Composition | Mixed solid and cystic | 1 |
| Echogenicity | Isoechoic and anechoic | 1 |
| Shape | Wider than taller | 0 |
| Margin | Smooth | 0 |
| Calcification | No | 0 |
| **Total** | | 2 |

- Total score: 2, TIRADS…II.

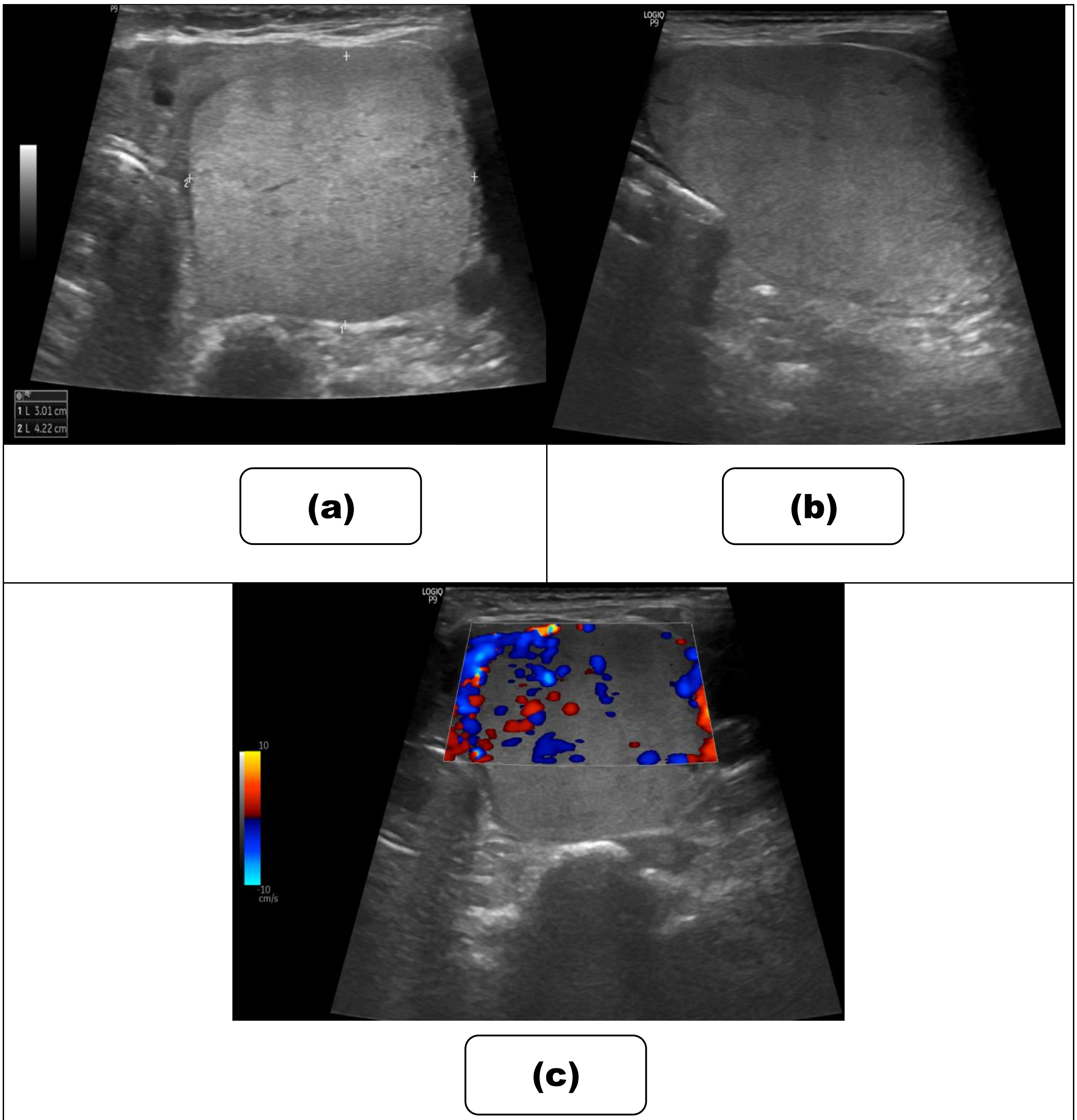


**Fig. (4):** Ultrasound images of follicular adenoma (a, b, c).

- Asymmetrically enlarged both thyroid lobes with multiple nodules, the most significant nodule measuring about 30x42 mm (AP x T).
- TIRAD classification:

| **Category** | **Comment** | **Score** |
|---|---|---|
| Composition | Solid | 2 |
| Echogenicity | Hyperechoic | 1 |
| Shape | Wider than taller | 0 |
| Margin | Smooth | 0 |
| Calcification | No calcifications | 0 |
| **Total** | | 3 |

- Total score: 3, TIRADS…III.

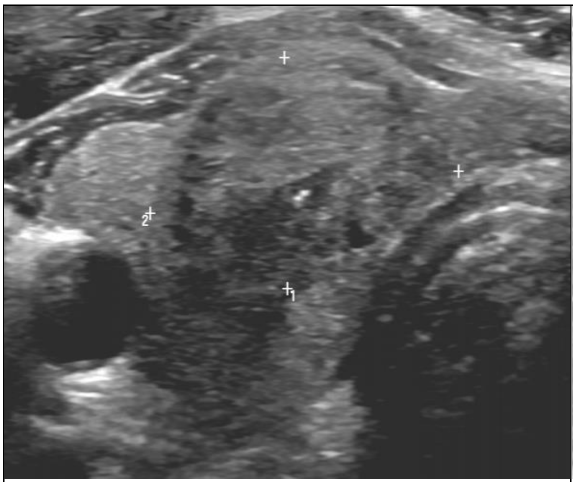

(a)

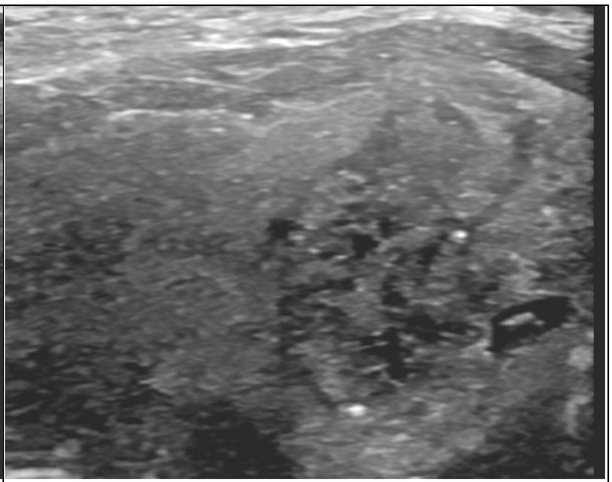

(b)

**Fig. (5):** Ultrasound images of B cell lymphoma (a, b).

- Enlarged right thyroid lobe with nodule measuring about 12x19 mm (AP x T).
- TIRAD classification:

| Category | Comment | Score |
|---|---|---|
| Composition | Mixed solid and cystic | 1 |
| Echogenicity | Isoechoic and anechoic | 1 |
| Shape | Wider than taller | 0 |
| Margin | Micro lobulated | 2 |
| Calcification | Micro calcifications | 3 |
| **Total** | | 7 |

- Total score: 7, TIRADS…V.

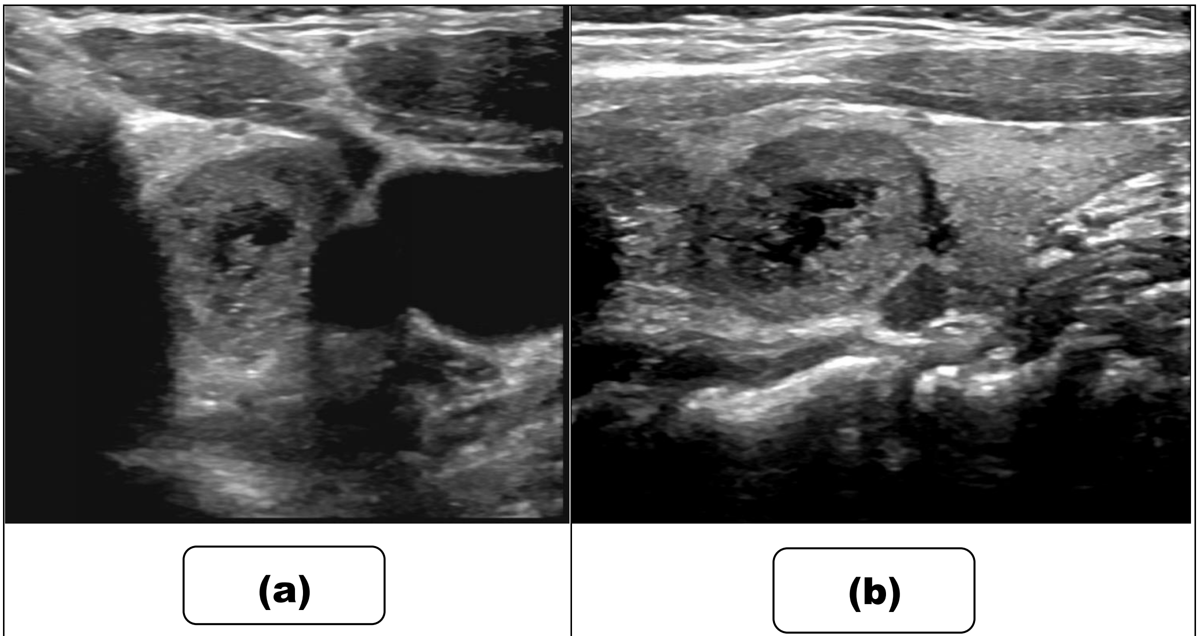


**Fig. (6):** Ultrasound images of follicular carcinoma (a, b).

- Enlarged left thyroid lobe with a nodule measuring about 15x10 mm (AP x T).
- TIRAD classification:

| **Category** | **Comment** | **Score** |
|---|---|---|
| Composition | Mixed solid and cystic | 1 |
| Echogenicity | Hypoechoic and anechoic | 2 |
| Shape | Taller than wider | 3 |
| Margin | Lobulated | 2 |
| Calcification | Micro calcifications | 3 |
| **Total** | | 11 |

- Total score: 11, TIRADS…V.

Regarding TIRAD categorization of our studied population, 15.7% were TIRAD 1, 11.4% were TIRAD 2, 17.1% were TIRAD 3, 18.6% were TIRAD 4 and 37.1% were TIRAD 5 (Table 2).

Table (2): Different pathological variants of thyroid nodules in correlation with TIRADS.

| Variant | TIRADS | | | | | Total | % |
|---|---|---|---|---|---|---|---|
| | I | II | III | IV | V | | |
| Lymphocytic thyroiditis | 2 | 4 | 1 | 1 | | 8 | 11.4% |
| Colloid nodule | 3 | 1 | 4 | 4 | | 12 | 17.1% |
| Follicular adenoma | 6 | 3 | 7 | 5 | | 21 | 30% |
| B-cell lymphoma | | | | | 2 | 2 | 2.9% |
| Medullary carcinoma | | | | | 2 | 2 | 2.9% |
| Papillary carcinoma on top of follicular adenoma | | | | | 4 | 4 | 5.7% |
| Follicular carcinoma | | | | | 7 | 7 | 10% |
| Papillary carcinoma | | | | 3 | 11 | 14 | 20% |
| **Total** | 11 | 8 | 12 | 13 | 26 | 70 | |
| **%** | 15.7% | 11.4% | 17.1% | 18.6% | 37.1% | | |

The 11 nodules in TIRADS 1 were pathologically proven benign. All 8 TIRADS 2 nodules were benign. Out of 12 TIRADS 3 nodules, all were benign. In the TIRADS 4 category, there were ten benign and three malignant nodules. Malignancy was proved in all TIRADS 5 nodules. When the final TI-RADS level increased from TR1 to TR5, there was a statistically significant (P value less than 0.001) increase in the probability of malignancy (Table 3).

Table (3): Correlation between TIRADS and pathology.

| Variant | Histopathological Results | |
|---|---|---|
| | Benign | Malignant |
| **TIRADS I** | 11 (26.8%) | 0 (0%) |
| **TIRADS II** | 8 (19.5%) | 0 (0%) |
| **TIRADS III** | 12 (29.3%) | 0 (0%) |
| **TIRADS IV** | 10 (24.4%) | 3 (10.3%) |
| **TIRADS V** | 0 (0%) | 26 (89.7%) |
| **Total** | 41 | 29 |

The ROC curve of the TI-RADS classification showed that the best cutoff point to detect malignant nodules regarding the TI-RADS total points score was five, which corresponds to the TR4 category with 80.80% sensitivity, 77% specificity, 72.5% positive predictive value, and 74.3% negative predictive value in the evaluation of thyroid lesions (Table 4 & Fig. 7).

Table 4: TIRADS score cutoff point, sensitivity, specificity, positive predictive value, and negative predictive value.

| Cut off point | Sensitivity | Specificity | +PV | -PV | Like hood test |
|---|---|---|---|---|---|
| TR4 | 80.80 | 77.00 | 72.5 | 74.3 | 0.467 |

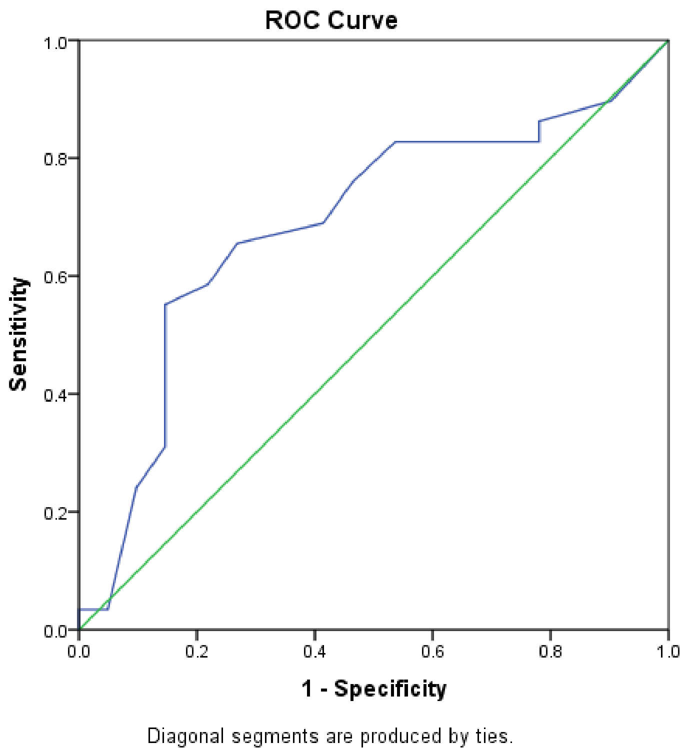


Fig. (7): Receiver operating characteristic (ROC) curve of TIRADS score in the studied group.

# Discussion

The most common abnormality of the thyroid gland is thyroid nodules. Thyroid nodules are fairly frequent radiological findings, either solid, cystic, or complex. The majority of nodules have a benign nature, and only about 5% are cancerous. **(13, 14)**

The differentiation between benign and malignant nodules is considered an important goal. In patients with benign nodules, it helps to avoid unnecessary surgery. Early detection of malignant nodules lowers disease mortality and morbidity rates. **(15)**

Ultrasound is more sensitive than MRI for detecting micro-lesions and identifying micro-calcification. **(15)**

Thyroid Imaging Reporting and Data System (TIRADS) is a scale for malignancy risk stratification. It aimed to develop evidence-based management recommendations for thyroid nodules based on well-defined ultrasonography characteristics that could be applied to any thyroid lesion**.** Following lesion grading, ultrasonography-guided FNAC is conducted on worrisome lesions, followed by histopathological analysis. (**16)**

Among our studied population, 42.9% were solid nodules, 31.4% were mixed cystic/solid, and 25.7% were spongiform. Echogenicity was hyper or isoechoic in 41.4%, anechoic and hypoechoic in 21.4% for each, and very hypoechoic in 15.7%. The shape was wider than tall in 71.4% and taller than wide in 28.6%. The margin was smooth/ill-defined in 37.1%, lobulated/irregular in 32.9%, and extra-thyroid extension was detected in 30%. Macro calcification was detected in 18.6%, peripheral calcification in 5.7%, and punctate calcification in 7.1%.

In the present study, 58.6% of the studied cases were benign lesions, and 41.4% were malignant, which agrees with **Ekinci et al. (2018),** who noted that the final pathological examinations revealed that 50 (76.9%) nodules made up the benign group, whereas 15 (23.1%) nodules made up the malignancy group.

In the current study, the most common lesion was benign follicular adenoma in 30%, followed by papillary thyroid carcinoma in 20%, then benign colloid nodule in 17.1%, lymphocytic thyroiditis in 11.4%, follicular carcinoma in 10%, papillary carcinoma on top of follicular adenoma in 5.7%, then each of B-cell lymphoma and medullary carcinoma in 2.9% which relatively near to the results in the study done by **(Noufal et al., 2018)** who found that the most common pathologies were follicular adenoma and colloid nodules, which accounted for around 2/3rd.

Regarding TIRAD categorization of our studied population, 15.7% were TIRAD 1, 11.4% were TIRAD 2, 17.1% were TIRAD 3, 18.6% were TIRAD 4 and 37.1% were TIRAD 5.

Among all the 11 nodules in TIRADS I were proven pathologically to be benign. All the eight thyroid nodules categorized TIRADS 2 were benign. All 12 nodules classified as TI-RADS 3 were benign. In the category of TIRADS 4, there were ten benign and three malignant nodules. All the 26 thyroid nodules classified as TIRADS 5 were malignant.

When the final TI-RADS category increased from TR1 to TR5, there was a statistically significant (P value less than 0.001) increase in the probability of malignancy.

This aligns with research conducted by **Barbosa TLM., et al., 2019** which found that patients with TR3 had a thyroid cancer risk of 23.3%, whereas TR-5 patients had a thyroid cancer rate of 38.5% of ACR-TIRADS. According to a different Indian study conducted in **2020 by De D. et al.,** TR-3 and TR-4 had 22% and 29% malignancy rates, respectively.

This is also in line with the findings of **Xu et al. (2017),** who observed that the probability of malignancy was 0% in TIRADS 1 and 2, 14.1% in TIRADS 3, 63.7% in TIRADS 4, and 100% in TIRADS 5.

In agreement with our results, studies by **Okasha H.H. et al., 2020** found that solid composition, hypoechoic echogenicity, irregular margin, microcalcifications, and taller-than-wide in shape significantly increased the risk of malignancy as these criteria raised the TIRADS total score points**.**

In this study, the ROC curve showed that the cutoff point to suspect malignant nodules regarding the TI-RADS total points score was five, which categorized TR4 with 80.80% sensitivity, 77% specificity,72.5% positive predictive value, and 74.3% negative predictive value in the evaluation of thyroid lesions. In the study done by **(Noufal et al., 2018) the** sensitivity and specificity of the study were 84.4% and 76.8%, respectively.

There are still some limitations in this study that affect the ability to differentiate between pathological subtypes of benign or malignant nodules. The relatively low percentage of certain pathological subtypes limits the statistical power and analytical results.

Furthermore, our study did not assess other criteria not included in the ACR TI-RADS, such as the existence of a peripheral halo, the pattern of vascularity, and the recently developed ultrasound elastography, which may aid in a more accurate characterization of thyroid nodules.

## Conclusion and recommendation

The ACR TI-RADS grading system makes thyroid nodule assessment easy and practical. It is simple to use in routine ultrasonography procedures and has high diagnostic accuracy in identifying malignant thyroid nodules.

The surgeon can determine the next course of action (biopsy or follow-up) based on TI-RADS since the degree of TI-RADS increases from TR1 to TR5, raising the overall risk of malignancy.

## Abbreviations

ACR: American collage of radiology

ADC: Apparent diffusion coefficient

EPI: Echo planner imaging

FNAC: Fine needle aspiration cytology

MRI: Magnetic resonance imaging

ROC: Receiver operating characteristics

ROI: Region of interest

SPSS: Statistical Package for the Social Sciences

STIR: Short tau inversion recovery

TE: Echo time

TR: Repetition time

# References


1. **Susana Calle, Jeanie Choi, Salmaan Ahmed, Diana Bell, &Kim O. Learned (2021).** Imaging of the thyroid. Neuroimaging Clinics. Volume 31, issue 3, P265-284.
2. **William D. Middleton, Sharlene A. Teefey, Carl C. Reading, Jill E. Langer, Michael D. Beland, and Terry S. Desser (2017).** Multi institutional Analysis of Thyroid Nodule Risk Stratification Using the American College of Radiology Thyroid Imaging Reporting and Data System. American Journal of Roentgenology.;208:1331-1341.10.2214/AJR.16.17613
3. **Tessler F.N., Middleton W.D., & Grant E.G. (2018).** Thyroid imaging reporting and data system (TI-RADS): a user's guide. Radiology, 287(1), 29-36.
4. **Trimboli P., &Giovanella L. (2016)** Thyroiditis. In: Giovanella L., Treglia G., Valcavi R. (eds) Atlas of Head and Neck Endocrine Disorders. Springer, Cham.
5. **Aleksandrov Y.K., Patrunov Y.N., & Sencha A.N. (2019).**Ultrasound-Guided Fine Needle Aspiration Biopsy. In: Sencha A., Patrunov Y. (eds) Thyroid Ultrasound. Springer, Cham.
6. **Moss W.J., Finegersh A., & Pang J. (2018).** Needle biopsy of routine thyroid nodules should be performed using a capillary action technique with 24- to 27-gauge needles: a systematic review and meta-analysis. Thyroid; 28 (7):857–63.
7. **Ehsan Seif, Mostafa Qorbani, Shaghayegh Mousavi, & Ali Salah Ashoor (2021).** A comparison of different Thyroid Imaging Reporting and Data Systems to reduce unnecessary FNAs and missed malignancies. Journal of Diagnostic Medical Sonography 1–8.
8. **Papini E., Persichetti A., Di Stasio E., Coccaro C., Graziano F., Bianchini A., et al. (2019).** OR27-1 Interobserver Agreement in the Assessement of Thyroid Nodules Ultrasound Features: A Blinded Multicenter Study. Journal of the Endocrine Society, 3(Supplement_1), OR27-21.
9. **Novosel T., & Jecker P. (2019).** Ultrasound of the Thyroid Gland. In Welkoborsky H. J. and Jecker P. (eds) Ultrasonography of the Head and Neck (pp. 259-278). Springer, Cham.
10. **Malhi H., Beland M.D., & Cen S.Y. (2014).** Echogenic foci in thyroid nodules: significance of posterior acoustic artifacts. AJR Am J Roentgenol 203(6):1310– 1316.
11. **ACR TI-RADS ATLAS TIRADS Classification. (2020).** Retrieved August 03, 2020, from https://arrangoizmd.com/tirads-classification.
12. **Monpeyssen H., & Tramalloni J. (2019).** The Role of Elastography in the Management of Thyroid Nodules In Luster M., Duntas L. H. & Wartofsky L. (eds) The Thyroid and Its Diseases (pp. 181-198). Springer, Cham.
13. **Germano A., Schmitt W., Carvalho M.R. & Marques R.M. (2019).** Normal ultrasound anatomy and common anatomical variants of the thyroid gland plus adjacent structures—A pictorial review. Clinical imaging, 58, 114-128.

14. **Rumack C.M. & Levine D. (2017).** Diagnostic ultrasound E-book. Elsevier Health Sciences.

15. **Luster M., Duntas L.H. & Wartofsky L. (2019).** Anatomy and Physiology of the Thyroid Gland. In Stathatos, N. (Ed.). The Thyroid and Its Diseases (pp. 3-12): Springer, Cham.

16. **Arrangoiz R., Cordera F., Caba D., Muñoz M., Moreno E., & de León E.L. (2018).** Comprehensive review of thyroid embryology, anatomy, histology, and physiology for surgeons. International Journal of Otolaryngology and Head & Neck Surgery, 7(4), 160-88.

17. **Ekinci, O., Boluk, S. E., Eren, T., Ozemir, I. A., Boluk, S., Salmaslioglu, A., ... & Alimoglu, O. (2018).** Diffusion-weighted magnetic resonance imaging for the detection of thyroid cancer. Cirugía Española (English Edition), 96(10), 620-626.

18. **Noufal, P., Ramakrishnan, K., Kurup, S., Ali, N., Janardhanan, S., Rabia, T.A., Unni, V., Bernaitis, L.J.J.o.E.o.M., Sciences, D. (2018).** Differntiation between benign and malignant thyroid nodule with diffusion weighted magnetic resonance imaging and apparent diffusion coefficient measurment and its histopathological correlation. 7, 843-850.

19. **Barbosa TLM., Junior COM., Graf H. (2019)**. ACR TI-RADS and ATA US scores are helpful for the management of thyroid nodules with indeterminate cytology. BMC Endocr Disord 19(1):1−11.

20. **De D., Dutta S., Tarafdar S. (2020)**. Comparison between sonographic features and fine needle aspiration cytology with histopathology in the diagnosis of solitary thyroid nodule. Indian J Endocrinol Metab 24(4):349.

21. **Xu T, Gu JY, Ye XH, Xu SH, Wu Y, Shao XY & Wu XH (2017).** Thyroid nodule sizes influence the diagnostic performance of TIRADS and ultrasound patterns of 2015 ATA guidelines: a multicenter retrospective study. Scientific reports, 7(1), 1-7.

22. **Okasha H.H., Mansor M., Sheriba N. (2020).** Role of elastography strain ratio and TIRADS score in predicting malignant thyroid nodule. Arch Endocrinol Metab 64 (6):735−742.